Journal of Pharmaceutical and Biomedical Analysis 53 (2010) 660–666

Contents lists available at ScienceDirect

Journal of Pharmaceutical and Biomedical Analysis

journal homepage: www.elsevier.com/locate/jpba

Characterization of interaction and the effect of carbamazepine on the structure of human serum albumin

Shankara S. Kalanur, J. Seetharamappa*, Veerendra Kumar A. Kalalbandi

Department of Chemistry, Karnatak University, Dharwad 580 003, India

ARTICLE INFO

Article history:
Received 15 February 2010
Received in revised form 26 May 2010
Accepted 26 May 2010
Available online 4 June 2010

Keywords:
Carbamazepine
Human serum albumin
Spectroscopic and voltammetric approach
Hydrophobic interactions
Site I of subdomain IIA

ABSTRACT

The binding of carbamazepine (CBZ) to human serum albumin (HSA) was investigated under simulative physiological conditions. In this study, intrinsic fluorescence of tryptophan-214 in HSA was monitored upon the addition of CBZ. Binding constant of CBZ–HSA was calculated by the remarkable static quenching effect of CBZ and found to be $(2.081 \pm 0.023) \times 10^4\ M^{-1}$. The fluorimetric results revealed that the hydrophobic interaction was a predominant intermolecular force for stabilizing the complex, which is also in agreement with the results obtained from voltammetric approach. Three site probes, warfarin, ibuprofen and digitoxin, were employed in fluorescence displacement experiments to locate the exact binding site for CBZ in HSA. The alteration in secondary structure of protein in the presence of CBZ was confirmed by the evidences from circular dichroism and FT-IR spectroscopy. Further, the distance *r* between donor (Trp-214) and acceptor (CBZ) was obtained according to fluorescence resonance energy transfer (FRET).

1. Introduction

Human serum albumin (HSA) is a principal extra cellular protein with a high concentration in blood plasma (40 mg ml^{-1} or 0.6 mM) [1]. HSA contributes to colloid osmotic blood pressure and is chiefly responsible for the maintenance of blood pH. It is known to play an important role in the transport and disposition of endogenous and exogenous ligands present in blood [1]. Its remarkable capacity to bind a variety of drugs results in its prevailing role in drug pharmacokinetics and pharmacodynamics. Its primary pharmacokinetics function is participating in absorption, distribution, metabolism and excretion of drug, of which the drug distribution is the one that HSA controls, because most drugs travel in plasma and reach the target tissues by binding to HSA [2]. Therefore, the studies on the interactions of a bioactive compound with HSA assume significance in chemistry, life sciences and clinical medicine.

CBZ, 5H-dibenzo[*b*,*f*]azepine-5-carbox-amide (Fig. 1), is a highly lipophilic neutral tricyclic compound. CBZ, as one of the most widely used antiepileptic drugs, is successfully prescribed in the treatment of psychomotor, generalized tonic–clonic seizures and complex partial seizures [3]. CBZ has been used as an anticonvulsant [4] and it has replaced both phenytoin and phenobarbitone as the first choice anticonvulsant for a number of pediatric seizure disorders. CBZ is usually administered at daily oral doses ranging from 200 to 1200 mg or more, which give rise to drug plasma levels of 4–12 mg ml^{-1} [5].

The reported HPLC methods [6–8] have not discussed the binding characteristics, binding sites, conformational changes etc of CBZ–HSA. In view of this, we planned to investigate the mode of mechanism, binding parameters, binding site and other details by spectroscopic and voltammetric techniques.

2. Experimental

2.1. Apparatus

Fluorescence measurements were performed on a Hitachi spectrofluorimeter Model F-7000 (Japan) equipped with a 150 W Xenon lamp and a slit width of 5 nm. Electrochemical studies were carried out using a CHI-1110a electrochemical Analyzer (CH Instruments Ltd. Co., USA, version 4.01) electrode system, including a GCE (3 mm diameter) as the working electrode, a platinum wire as a counter electrode and an Ag/AgCl (3 M KCl) as reference electrode. The CD measurements were made on a JASCO-J-715 spectropolarimeter using a 0.1 cm cell at 0.2 nm intervals, with three scans averaged for each CD spectrum in the range of 200–250 nm. The infrared spectra were acquired on a Thermo Nicolet-5700 FT-IR spectrometer (Waltham, MA, USA) equipped with a germanium attenuated total reflection (ATR) accessory, a DTGS KBr detector and a KBr beam splitter. All spectra were recorded via the ATR method with a resolution of 4 cm^{-1} and 60 scans. The absorption spectra were recorded on a double beam CARY 50-BIO UV–vis spectropho-

* Corresponding author. Tel.: +91 836 2215286; fax: +91 836 2747884.
E-mail address: jseetharam@yahoo.com (J. Seetharamappa).

0731-7085/$ – see front matter © 2010 Elsevier B.V. All rights reserved.
doi:10.1016/j.jpba.2010.05.025

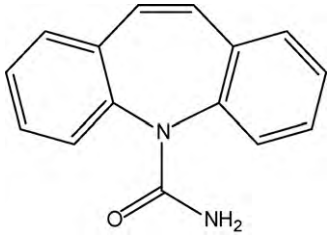

Fig. 1. Structure of CBZ.

tometer equipped with a 150 W Xenon lamp and a slit width of 5 nm.

2.2. Reagents

HSA was obtained from Sigma Chemical Company, St Louis, USA. A stock solution of 250 μM HSA was prepared in phosphate buffer of pH 7.4 containing 0.15 M NaCl based on its molecular weight of 66,000. A stock solution of CBZ (250 μM) was prepared in phosphate buffer–acetonitrile mixture (80:20). Solutions of metal cations were prepared from their respective metal chlorides. Under the experimental conditions, no cation gave precipitate in phosphate buffer. Stock solutions of warfarin, ibuprofen and digitoxin (each of 250 μM) were prepared by dissolving first in minimum amount of alcohol and then diluting with phosphate buffer of pH 7.4 containing 0.15 M NaCl.

2.3. Procedures

2.3.1. Fluorescence quenching study

Based on preliminary experiments, the concentration of HSA was kept fixed at 5 μM while that of CBZ was varied from 5 to 55 μM. Fluorescence spectra were recorded at 293, 298, 303 and 307 K in the range of 290–500 nm upon excitation at 280 nm in each case.

2.3.2. Voltammetric characterization of interaction of CBZ with HSA

For voltammetric studies, the concentration of CBZ was maintained constant (10 μM) while that of HSA was varied (0–50 μM). A given CBZ–HSA system was stirred for 60 s and then, differential pulse voltammogram was recorded (scanning potential: from 0.7 to 1.6 V; sweep rate: 100 mV s^{-1}).

2.3.3. Circular dichroism measurements

The CD spectra of HSA in the range of 200–250 nm in the absence and presence of CBZ were recorded by keeping the concentration of HSA at 5 μM and varying concentration of drug from 0 to 50 μM.

2.3.4. FT-IR measurements

The FT-IR spectra of HSA (5 μM) in presence and absence of CBZ were recorded ($n = 3$ replicates) in the range of 1500–1750 cm^{-1}. The corresponding absorbance contributions of buffer and free CBZ solutions were recorded and digitally subtracted with the same instrumental parameters.

2.3.5. UV absorption studies

The UV measurements of HSA in the presence and absence of CBZ were made in the range of 200–310 nm. The concentration of HSA was fixed at 5 μM while that of drug was varied from 0 to 20 μM.

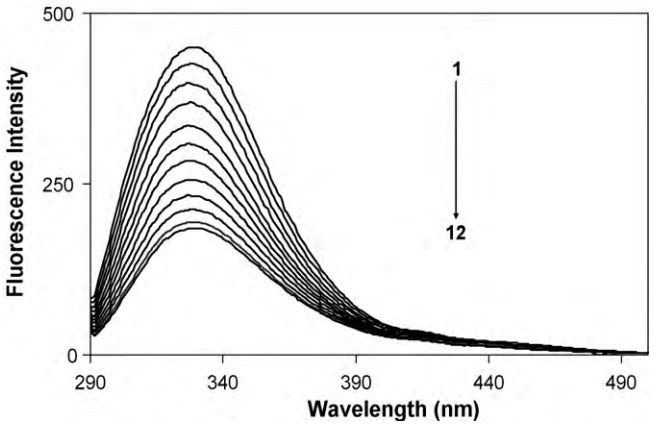

Fig. 2. Fluorescence emission spectra of HSA (5 μM) with various amounts of CBZ following the excitation at 280 nm. 1–12 indicate the spectra recorded at [CBZ] = 0, 5, 10, 15, 20, 25, 30, 35, 40, 45, 50 and 55 μM.

2.3.6. Effects of some common ions

The fluorescence spectra of CBZ (5–55 μM)–HSA (5 μM) were recorded in presence and absence of various common ions (each of 5 μM) *viz.*, Fe^{3+}, Co^{2+}, K^{+}, Ni^{2+}, Ca^{2+}, Zn^{2+}, Mn^{2+} and Cu^{2+} in the range of 300–500 nm upon excitation at 280 nm.

3. Results and discussion

3.1. Fluorescence quenching mechanism

HSA has a single tryptophan residue (Trp-214) located in the hydrophobic cavity of the subdomain IIA corresponding to the so-called Sudlow's drug binding site I region [9]. The intrinsic fluorescence of the unique tryptophan is very sensitive to the environment around the amino acid residues. Binding of small molecules with HSA sometimes induces changes in protein conformation and consequently its fluorescence. Therefore, fluorescence of Trp-214 has been employed frequently in the study of interaction of protein with drugs [10]. Hence, the interaction of CBZ with HSA was investigated by monitoring Trp-214 fluorescence in the titration experiment. The addition of CBZ to HSA resulted in substantial change in the fluorescence of Trp-214 (Fig. 2).

It is evident from Fig. 2 that the fluorescence intensity of HSA decreased gradually as concentration of CBZ increased from 0 to 55 μM. In addition to the decrease in fluorescence intensity, the wavelength of peak was noticed to be shifted to lower wavelength. This indicated the increased hydrophobicity around tryptophan [11]. The drop in tryptophan fluorescence can also be rationalized by assuming conformational changes in the protein after binding to CBZ.

Fluorescence quenching refers to any process which decreases the fluorescence intensity of a sample. A variety of molecular interactions can result in quenching including excited-state reactions, molecular rearrangements, energy transfer, ground-state complex formation and collisional quenching. The different mechanisms of quenching are usually classified as either dynamic or static quenching. Dynamic and static quenching can be distinguished by their differing dependence on temperature and viscosity. Dynamic quenching depends upon diffusion. Since higher temperatures result in larger diffusion coefficients, the bimolecular quenching constants are expected to increase with increasing temperature. In contrast, increased temperature is likely to result in decreased stability of complexes and thus lower values of the static quenching constants. In order to speculate the fluorescence quenching mechanism, the fluorescence quenching data at different temperatures (293, 298, 303 and 307 K) were firstly analyzed using the classical

Table 1
Modified Stern–Volmer association constant, binding constants and binding sites of CBZ–HSA system.

Temperature (K)	K_a (l mol^{-1})	Correlation coefficient	Binding constant (M^{-1})	Number of binding sites (n)	Correlation coefficient
293	$(1.301 \pm 0.021) \times 10^4$	0.9745	$(2.394 \pm 0.017) \times 10^4$	1.031 ± 0.011	0.9788
298	$(1.276 \pm 0.033) \times 10^4$	0.9715	$(2.081 \pm 0.023) \times 10^4$	1.015 ± 0.007	0.9814
303	$(1.222 \pm 0.028) \times 10^4$	0.9821	$(1.813 \pm 0.019) \times 10^4$	1.055 ± 0.015	0.9863
307	$(1.098 \pm 0.015) \times 10^4$	0.9755	$(1.621 \pm 0.031) \times 10^4$	0.983 ± 0.021	0.9945

Stern–Volmer equation [12]. The Stern–Volmer quenching constant, K_{SV} values were calculated (not shown) and in turn evaluated the values of quenching rate constant, k_q at different temperatures. Higher k_q values compared to the maximum value reported for a diffusion controlled process ($K_{dif} = 2.0 \times 10^{10}$ M^{-1} s^{-1}) [13] revealed the formation of complex rather than dynamic mechanism. Therefore, the quenching data were subjected to the modified Stern–Volmer equation given below [14]:

$$\frac{F_0}{\Delta F} = \left\{\frac{1}{f_a K_a [Q]}\right\} + \left(\frac{1}{f_a}\right) \quad (1)$$

where F_0 is the fluorescence intensity in the absence of quencher (CBZ), ΔF is the difference in fluorescence in the absence and presence of the quencher (CBZ) at concentration [Q], K_a is the modified Stern–Volmer association constant, and f_a is the effective quenching constant for the accessible fluorophores. The plot of $F_0/\Delta F$ *versus* 1/[Q] yielded $1/f_a$ as the intercept, and $1/(f_a K_a)$ as the slope. The values of Stern–Volmer association constants K_a were evaluated and are shown in Table 1. The decreasing trend of K_a with increase in temperature indicated the presence of static quenching mechanism (and hence formation of complex).

3.2. Binding constant and the number of binding sites

When small molecules bind independently to a set of equivalent sites on a macromolecule, then the equilibrium between free and bound molecules is given by the following equation [15]:

$$\frac{\log(F_0 - F)}{F} = \log K + n \log[Q] \quad (2)$$

where K is the binding constant and n is the number of binding sites per albumin molecule. The binding constant and the number of binding sites were calculated from the plot of $\log(F_0 - F)/F$ *versus* $\log[Q]$ and are shown in Table 1. It can be inferred from the values of n that there is one independent class of binding sites on HSA for CBZ. The value of K illustrated that there is a strong binding force between CBZ and HSA. It was found that the binding constant decreased with increase in temperature resulting in a reduction of the stability of the CBZ–HSA complex.

3.3. Thermodynamic parameters and binding modes

Generally, small molecular substrates bind to protein through binding forces *viz*., van der Waals interaction, hydrophobic force, electrostatic interaction and hydrogen bond. The thermodynamic parameters, enthalpy change (ΔH^0), entropy change (ΔS^0) and free energy change (ΔG^0) of interaction are the main evidences for confirming the binding mode. In order to elucidate the interaction of CBZ with HSA, these thermodynamic parameters were calculated. The temperature dependence of the binding was studied at 293, 298, 303 and 307 K. HSA did not undergo any structural degradation since the temperature effect is very small; the interaction enthalpy change can be regarded as constant if the temperature range is not too wide. The thermodynamic parameters are evaluated using the following equations:

$$\log K = \frac{-\Delta H^0}{2.303RT} + \frac{\Delta S^0}{2.303R} \quad (3)$$

Table 2
Thermodynamic parameters of CBZ–HSA interaction at pH 7.4.

Temperature (K)	ΔH^0 (kJ mol^{-1})	ΔS^0 (J mol^{-1} K^{-1})	ΔG^0 (kJ mol^{-1})
293	−19.76	15.58	−24.57
298			−24.64
303			−24.71
307			−24.82

and

$$\Delta G^0 = \Delta H^0 - T\Delta S^0; \quad \Delta G^0 = -2.303RT \log K \quad (4)$$

From the plot of $\log K$ *versus* $1/T$ the values of ΔH^0 and ΔS^0 were found to be −19.76 and 15.58 J mol^{-1} K^{-1}, respectively (Table 2). Negative ΔH^0 and positive ΔS^0 values indicated that the binding process is exothermic. Further, the negative values of ΔG^0 indicated spontaneity of the binding of CBZ to HSA. For drug–protein interaction, the positive ΔS^0 is frequently taken as evidence for the hydrophobic interaction [16] because the water molecules that are arranged in an orderly fashion around the ligand and protein acquire a more random configuration. In this way, the destruction of the water structure was induced by hydrophobic interactions [16]. The negative ΔH^0 and positive ΔS^0 values, therefore, showed that the hydrophobic interactions played a major role in the binding of CBZ to HSA.

3.4. Voltammetric study of interaction of CBZ with HSA

One of the applications of the electroanalytical technique includes its utility to study the interaction of macromolecule with small molecules. Differential pulse voltammogram (DPV) of CBZ showed two oxidation peaks at 1.156 and 1.344 V in phosphate buffer of pH 7.4. Detailed voltammetric study revealed that the peak 1 (at 1.156 V) is diffusion controlled while peak 2 (at 1.344 V) is adsorption controlled. In order to investigate the interaction of CBZ with HSA, known amounts of HSA were added to fixed concentration of CBZ solution and DPV were recorded. Both oxidation peaks of CBZ were observed to be shifted towards higher potential with decrease in oxidation peak current. The DPV of CBZ in presence and absence HSA are shown in Fig. 3.

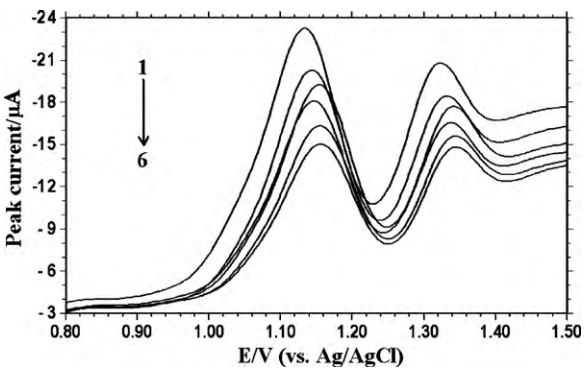

Fig. 3. DPV of CBZ in presence of HSA. CBZ concentration was maintained at 10 μM and HSA concentrations were (1) 0, (2) 10, (3) 20, (4) 30, (5) 40 and (6) 50 μM.

With increase in concentration of HSA, decreased peak currents were observed. These observations suggested the formation of a non-electroactive CBZ–HSA complex. Further, it was proposed that the decrease in peak current is mainly due to decrease in free concentration of CBZ (due to complex formation between CBZ and HSA) but not due to the factors like, alteration in electrochemical kinetics of CBZ due to addition of HSA or the blockage of the electrode surface or adsorption of HSA on the electrode or competitive adsorption between CBZ and HSA on GCE. The observed potential shift in the oxidation peak was attributed to hydrophobic interaction between CBZ and HSA [17]. This result is in agreement with the observation made by spectroscopic techniques. So, it is proposed that the interaction occurred between the most hydrophobic segment of the CBZ molecule and the hydrophobic part of the HSA cavity.

Assuming that the interaction of CBZ with HSA produces only a single HSA–*m*CBZ complex, the number of binding sites, *m*, and the binding constant, β_S, are deduced using the equation shown below [18]:

$$\log\left[\frac{\Delta I}{\Delta I_{max} - \Delta I}\right] = \log \beta_S + m \log[\text{CBZ}] \quad (5)$$

where ΔI is the difference in peak current in presence and absence of HSA and ΔI_{max} corresponds to the value obtained when the concentration of CBZ is extremely higher than that of HSA. C_{HSA}, [HSA] and [HSA–*m*CBZ] correspond to the total, free and bound concentration of protein in the solution, respectively.

For this, the concentration of CBZ was kept constant (10 μM) and that of HSA was varied in the range of 0–50 μM. If HSA interacts with CBZ to form a single complex, then the plot of log $[\Delta I/(\Delta I_{max} - \Delta I)]$ *versus* log [CBZ] shows linearity. The values of binding ratio and binding constant are obtained from the slope and intercept of this plot. Thus, the resulting linear plot ($r = 0.9961$) gave the value of m to be 1.02 ± 0.05 and that of β_S to be $(2.234 \pm 0.089) \times 10^4\ M^{-1}$. The value of binding constant is in close agreement with that obtained by spectroscopic technique $(2.081 \pm 0.023) \times 10^4\ M^{-1}$. The binding ratio of 1.02 indicated that 1 mole of CBZ interacted with 1 mole of HSA. This also indicated the presence of single class of binding sites on HSA for CBZ.

3.5. Energy transfer between CBZ and HSA

It is known that the technique of fluorescence resonance energy transfer (FRET) is useful for measuring the distance between the donor fluorophore and acceptor *in vitro* and *in vivo* [19]. It is a non-destructive spectroscopic method that can be employed to monitor the proximity and relative angular orientation of the donor and acceptor. Transfer of energy may take place through a direct electrodynamic interaction between the primarily excited molecule and its neighbors, which will take place under the following conditions: (i) the donor can produce fluorescence light; (ii) fluorescence emission spectrum of the donor and UV–vis absorbance spectrum of the acceptor have more overlap; and (iii) the distance between the donor and the acceptor is lower than 8 nm [20]. According to the Förster's theory, the energy transfer efficiency, *E* was calculated using the following equation [19]:

$$E = 1 - \left(\frac{F}{F_0}\right) = \frac{R_0^6}{R_0^6 + r^6} \quad (6)$$

where F and F_0 are the fluorescence intensities of HSA in presence and absence of CBZ; r is the distance between the protein and CBZ, and R_0 is the Förster critical distance at which 50% of the excitation energy is transferred to the acceptor [21]. The value of R_0 can be deduced using the equation shown below:

$$R_0^6 = 8.8 \times 10^{-25} K^2 N^{-4} \Phi J \quad (7)$$

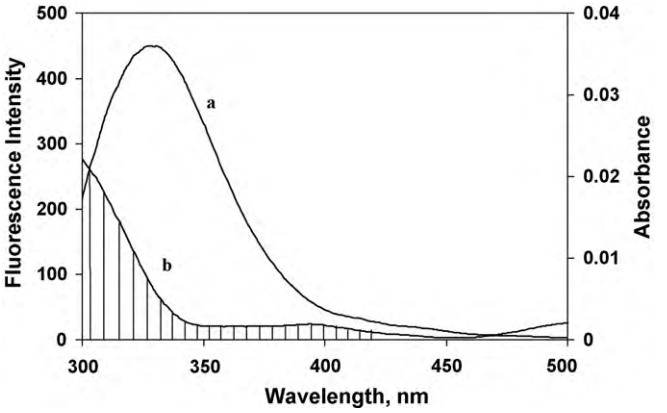

Fig. 4. The overlap of fluorescence emission spectrum of HSA (a) with the UV absorption spectrum of CBZ (b). [CBZ] = [HSA] = 5 μM.

where K^2 is the spatial orientation factor of the dipole, N is the refractive index of the medium, Φ is the fluorescence quantum yield of the donor and J is the overlap integral of the fluorescence emission spectrum of the donor and absorption spectrum of the acceptor. J is given by

$$J = \frac{\int_0^\infty F(\lambda)\varepsilon(\lambda)\lambda^4 \Delta\lambda}{\int_0^\infty F(\lambda)\Delta\lambda} \quad (8)$$

where $F(\lambda)$ is the fluorescence intensity of the fluorescent donor at wavelength λ, $\varepsilon(\lambda)$ is the molar absorption coefficient of the acceptor at wavelength λ. From the above relationships, J, E, R_0 and r can be calculated. Fig. 4 showed the overlap of the fluorescence spectrum of HSA with the absorption spectrum of CBZ.

For this, equimolar concentrations of CBZ and HSA were employed. The overlap integral, J in Eq. (8) can be calculated by integrating the spectrum shown in Fig. 4. The value of J was calculated to be $3.16 \times 10^{-15}\ cm^3\ l\ mol^{-1}$. Using the values of $K^2 = 2/3$, $N = 1.333$ and $\Phi = 0.118$ [22], the values of R_0 and r were found to be 2.91 and 3.43 nm, respectively. An essential criterion for energy transfer to take place is that the distance between donor and acceptor must be within 2–8 nm. This criterion is satisfied in the above case and hence quenching of tryptophan fluorescence of HSA in the presence of probe is attributed to energy transfer. The higher value of r compared to the value of R_0 revealed the presence of static quenching mechanism [23]. The shorter distance between the bound CBZ and tryptophan residues in the proposed study suggested the significant interaction between CBZ and HSA.

3.6. Displacement experiments with site markers

HSA is composed of three domains I, II and III which confer to the protein a heart shaped molecular form [24]. Each domain is constituted by two subdomains. The subdomains share a number of common features, such as the hydrophobic face, the cluster of basic amino acid residues and proline residues at the tips of the long loops. However, it is known that each subdomain is also unique and probably exhibits a certain degree of binding specificity. Sudlow have suggested that the HSA has two distinct binding sites *viz.*, sites I and II [25]. Site I of HSA has affinity for warfarin, phenylbutazone, etc., while site II shows affinity for ibuprofen, flufenamic acid, etc. Digitoxin binding is independent of sites I and II. In order to determine the specificity of CBZ binding, competition experiments were performed with warfarin, ibuprofen and digitoxin.

The displacement experiments were performed by keeping the concentration of HSA and the site probe constant (each of 5 μM). The fluorescence intensity of HSA-probe was recorded in presence

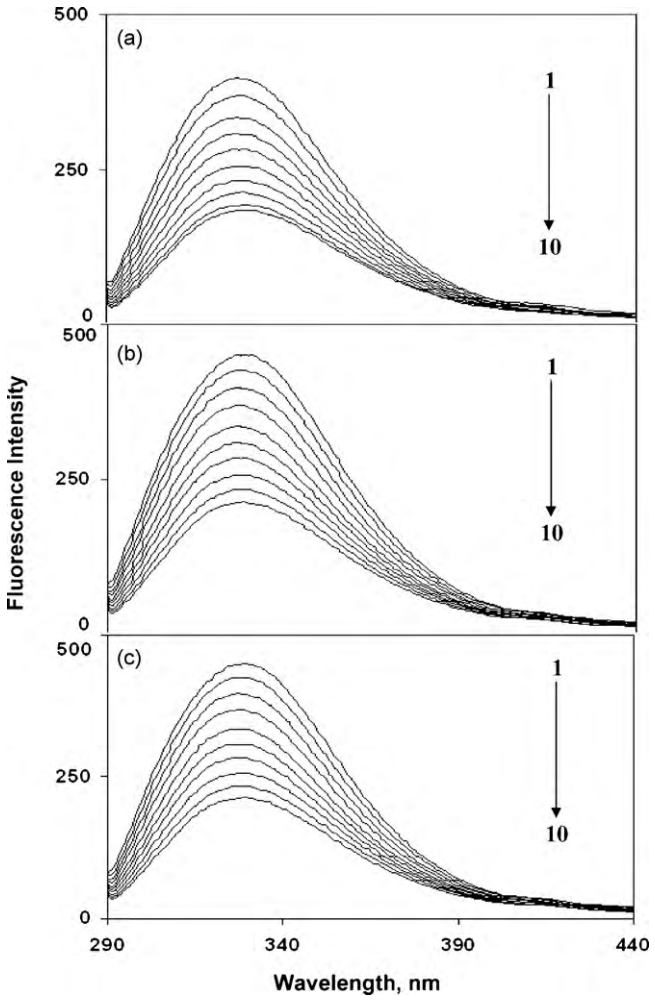

Fig. 5. Fluorescence emission spectra of CBZ–HSA in presence of site probes. In this, site probes refer to warfarin (a), ibuprofen (b) and digitoxin (c). The concentrations of HSA and site probes were maintained constant at 5 μM while that of CBZ was varied: (1) 0, (2) 5, (3) 10, (4) 15, (5) 20, (6) 25, (7) 30, (8) 35, (9) 40 and (10) 45 μM.

of increasing amounts of drug and the corresponding results are shown in Fig. 5.

The binding constant values of CBZ–HSA were observed to be $(1.25 \pm 0.16) \times 10^4\,M^{-1}$, $(2.09 \pm 0.22) \times 10^4\,M^{-1}$ and $(2.10 \pm 0.19) \times 10^4\,M^{-1}$ in presence of warfarin, ibuprofen and digitoxin, respectively. It was observed that the binding constant of CBZ–HSA decreased markedly in presence of warfarin indicating the competition between warfarin and CBZ for site I of subdomain IIA. No significant effects were observed in presence of ibuprofen and digitoxin. This revealed that these two site markers did not compete with CBZ for same binding site on HSA. Hence, the site I located in subdomain IIA near Trp-214 is proposed to be the main binding site for CBZ in HSA.

3.7. Conformational investigation of serum albumin

3.7.1. CD spectra

To ascertain the possible influence of drug binding on the secondary structure of HSA, we have carried out CD studies in the presence of different concentrations of CBZ. The CD spectra of HSA exhibited two negative bands in the far-UV region at 208 and 220 nm (Fig. 6), which are characteristics of α-helix structure in protein [26].

These peaks are attributed to $n-\pi^*$ transition for the peptide bond of α-helix. Addition of CBZ to HSA caused only a subtle

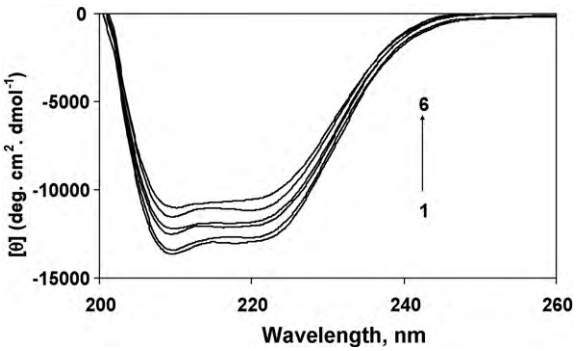

Fig. 6. CD spectra of the CBZ–HSA system at 298 K. [HSA] = 5 μM; CBZ to HSA ratios: (1) 0:1, (2) 2:1, (3) 4:1, (4) 6:1, (5) 8:1 and 10:1.

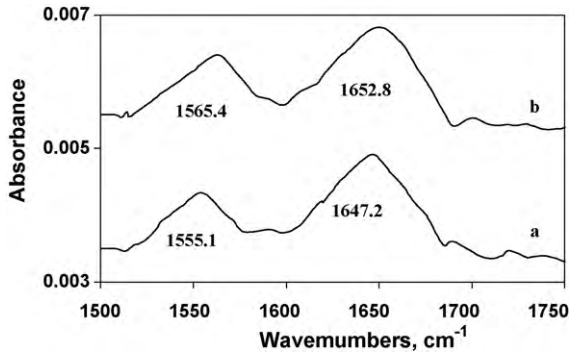

Fig. 7. FT-IR spectra and different spectra of HSA in buffer of pH 7.4: (a) FT-IR spectrum of HSA and (b) FT-IR difference spectrum of HSA obtained by subtracting the spectrum of the CBZ-free form from that of the CBZ-bound form in the region of 1750–1500 cm^{-1}.

decrease in negative ellipticity in far-UV CD region without any significant shift of peaks. The α-helix contents of free and combined HSA were calculated from mean residue ellipticity values at 208 nm using the following equations:

$$\text{MRE} = \frac{\text{observed CD(m}deg\text{)}}{C_p n l \times 10} \tag{9}$$

$$\alpha\text{-Helix}\,(\%) = \left[\frac{-\text{MRE}_{208} - 4000}{33,000 - 4000}\right] \times 100 \tag{10}$$

where n is the number of amino acid residues in protein, l is the path length and C_p is the concentration of protein. From the above equation, the α-helicity in the secondary structure of HSA was determined and found to be decreased from 57.03 ± 0.21, % in free HSA to 52.91 ± 0.39, % in the CBZ–HSA complex, which was indicative of the loss of α-helicity upon interaction. However, the shape of peaks and the peak maximum position remained almost same. This indicated that the HSA has predominantly α-helix nature even after binding to the drug.

3.7.2. FT-IR spectra

Infrared spectra of proteins exhibit a number of amide bands, which represent different vibrations of the peptide moieties. Of all the amide modes of the peptide group, the amide I is the most widely used one in studies of protein secondary structure. This vibration mode originates from the C=O stretching vibration of the amide group (coupled to the in-phase bending of the N–H bond and the stretching of the C–N bond) and gives rise to infrared bands in the region between 1600 and 1700 cm^{-1} [27]. Further, to prove the conformational changes in HSA induced by the binding of CBZ to HSA, we have recorded the FT-IR spectra of HSA and CBZ–HSA complex (Fig. 7).

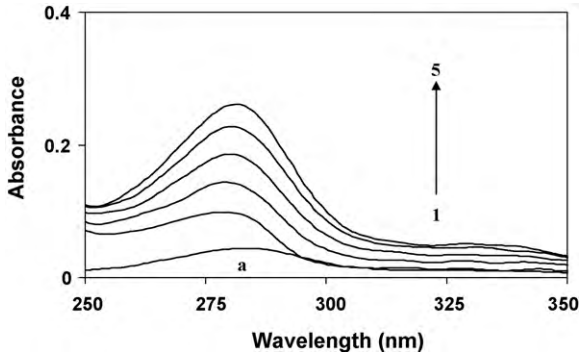

Fig. 8. UV–vis absorption spectra of 5 μM HSA (1) in presence of increasing concentration of CBZ (1) 0, (2) 5, (3) 10, (4) 15 and (5) 20 μM. (a) Indicates 5 μM of CBZ only.

The FT-IR spectrum of free HSA was acquired by subtracting the absorption of phosphate buffer from the spectrum of protein solution, which exhibited the characteristic amide I and amide II absorption bands at 1647.2 and 1555.1 cm^{-1}, respectively. The difference spectrum of HSA was obtained by subtracting the spectrum of CBZ-free form from that of CBZ-bound form. It was clear that the amide I and amide II bands shifted from 1647.2 to 1652.8 cm^{-1} and from 1555.1 to 1565.4 cm^{-1}, respectively. This indicated the change in secondary structure of HSA upon binding to CBZ.

3.7.3. UV–vis absorption studies

The UV absorption spectra of CBZ, HSA and CBZ–HSA are shown in Fig. 8.

It is evident that the absorbance of HSA increased regularly with increase in the concentration of CBZ. Moreover, the maximum peak position of CBZ–HSA was observed to be shifted slightly towards higher wavelength region. This change in λ_{max} indicated the change in polarity around the tryptophan residue and the change in peptide strand of HSA molecules and hence the change in hydrophobicity. This indicated that the binding between CBZ and protein molecule has led to changes in protein conformation.

3.7.4. The effect of cations on the binding of CBZ to HSA

The binding of cations to proteins is of great interest in biological science (for catalytic function and structural stability) and a good understanding of this relationship is needed for the control of the structure and functionality of proteins. The multiple binding sites underlie the exceptional ability of HSA to interact with many organic and inorganic molecules and make this protein an important regulator of intercellular fluxes and the pharmacokinetic behavior of many drugs. The effect of common ions on the binding of CBZ to HSA was investigated at 298 K. The corresponding binding constant values are shown in Table 3. It is evident from Table 3 that the binding constant of CBZ–HSA increased marginally in the presence of Cu^{2+}. This indicated stronger binding between CBZ and HSA. Further, this prolonged the storage time of drug in blood plasma that could enhance the maximum effectiveness of the drug. Therefore, CBZ could be stored and transported better by the proteins in the presence of Cu^{2+}. In presence of K^+, Co^{2+}, Ni^{+2}, Ca^{2+}, Mn^{2+}, Fe^{3+} and Zn^{2+}, the binding constant of CBZ–HSA decreased to various degrees. This indicated that the presence of these ions reduced the CBZ–HSA binding, causing CBZ to be quickly cleared from the blood, which might lead to the need for more doses of CBZ to achieve the desired medicinal effect [28].

Table 3
Effects of some cations on binding of CBZ to HSA at 298 K.

System	Binding constant for CBZ–HSA (M^{-1})
CBZ + HSA	$(2.081 \pm 0.023) \times 10^4$
CBZ + HSA + K^+	$(2.081 \pm 0.019) \times 10^4$
CBZ + HSA + Ni^{2+}	$(1.437 \pm 0.031) \times 10^4$
CBZ + HSA + Co^{2+}	$(1.673 \pm 0.019) \times 10^4$
CBZ + HSA + Cu^{2+}	$(2.293 \pm 0.037) \times 10^4$
CBZ + HSA + Fe^{3+}	$(2.080 \pm 0.023) \times 10^4$
CBZ + HSA + Zn^{2+}	$(0.985 \pm 0.028) \times 10^4$
CBZ + HSA + Ca^{2+}	$(1.694 \pm 0.015) \times 10^4$
CBZ + HSA + Mn^{2+}	$(1.324 \pm 0.011) \times 10^4$

4. Conclusions

This work provides a valuable information about the interaction of an antidepressant, CBZ with HSA. We have employed various spectroscopic (Fluorescence, UV–vis absorption, CD and FT-IR spectroscopy) and voltammetric techniques to probe the binding of CBZ to HSA. The studies showed that CBZ quenched the intrinsic fluorescence of HSA through static quenching mode and hydrophobic interactions played a major role in the interaction. The experimental results indicated that CBZ interacted with HSA strongly at site I (subdomain IIA). The α-helical content of protein was found to decrease upon binding to CBZ.

Acknowledgements

We are grateful to the Council of Scientific and Industrial Research, New Delhi, for financial assistance (No. 01(2279)/08/EMR-II dated 20-11-2008). We thank Head, Department of Molecular Biophysics, Indian Institute of Science, Bangalore, for CD measurement facilities. Thanks are also due to the authorities of the Karnatak University, Dharwad, for providing the necessary facilities.

References

[1] D.C. Carter, J.X. Ho, Structure of serum albumin, Adv. Protein Chem. 45 (1994) 153–203.
[2] F. Herve, S. Urien, E. Albengres, J.C. Duche, J.P. Tillement, Drug binding in plasma. A summary of recent trends in the study of drug and hormone binding, Clin. Pharmacokinet. 26 (1994) 44–58.
[3] J. Mc Numara, Goodman and Gilman's The Pharmacological Basis of Therpeutics, Tenth edn., McGraw-Hill, New York, 2001.
[4] I. Bernus, R.G. Dickinson, W.D. Hooper, M.J. Eadie, Dose-dependent metabolism of carbamazepine in humans, Epilepsy Res. 24 (1996) 163–172.
[5] R.H. Mattson, Efficacy and adverse effects of established and new antiepileptic drugs, Epilepsia 36 (2007) 13–26.
[6] H.S. Kim, I.W. Wainer, Rapid analysis of the interactions between drugs and human serum albumin (HSA) using high-performance affinity chromatography (HPAC), J. Chromatogr. B 870 (2008) 22–26.
[7] H.S. Kim, D.S. Hage, Chromatographic analysis of carbamazepine binding to human serum albumin, J. Chromatogr. B 816 (2005) 57–66.
[8] H.S. Kim, R. Mallik, D.S. Hage, Chromatographic analysis of carbamazepine binding to human serum albumin II. Comparison of the Schiff base and *N*-hydroxysuccinimide immobilization methods, J. Chromatogr. B 837 (2006) 138–146.
[9] J.R. Brown, Serum albumin: amino acid sequence, in: V.M. Rosenoer, M. Oratz, M.A. Rothschild (Eds.), Albumin Structure, Function and Uses, Pergamon Press, Oxford, 1977.
[10] H.M. Ma, X. Chen, N. Zhang, Y.Y. Han, D. Wu, B. Du, Q. Wei, Spectroscopic studies on the interaction of a water-soluble cationic porphyrin with proteins, Spectrochim. Acta A 72 (2009) 465–469.
[11] J.R. Lakowicz, Principles of Fluorescence Spectroscopy, Plenum Press, New York, 2006.
[12] M.R. Eftink, Biophysical and Biochemical Aspects of Fluorescence Spectroscopy, Plenum Press, New York, 1991.
[13] J.R. Lakowicz, G. Weber, Quenching of fluorescence by oxygen. A probe for structural fluctuations in macromolecules, Biochemistry 12 (1973) 4161–4170.
[14] M.M. Yang, X.L. Xi, P. Yang, Study of the interaction of cephalosporin class medicine with albumin by fluorescence enhancement and fluorescence quenching theories, Chin. J. Chem. 24 (2006) 642–648.
[15] X.Z. Feng, Z. Lin, L.J. Yang, C. Wang, C.L. Bai, Investigation of the interaction between acridine orange and bovine serum albumin, Talanta 47 (1998) 1223–1229.
[16] P.D. Ross, S. Subramanian, Thermodynamics of protein association reactions: forces contributing to stability, Biochemistry 20 (1981) 3096–3102.

[17] H. Heli, N. Sattarahmady, A. Jabbari, A.A. Moosavi-Movahedi, G.H. Hakimelahi, F.Y. Tsai, Adsorption of human serum albumin onto glassy carbon surface-applied to albumin-modified electrode: mode of protein–ligand interactions, J. Electroanal. Chem. 610 (2007) 67–74.
[18] W. Sun, K. Jiao, Linear sweep voltammetric determination of protein based on its interaction with Alizarin Red S, Talanta 56 (2002) 1073–1080.
[19] T. Förster, 10th Spiers Memorial Lecture. Transfer mechanisms of electronic excitation, Discuss. Faraday Soc. 27 (1959) 7–17.
[20] B. Valeur, J.C. Brochon, New Trends in Fluorescence Spectroscopy, Springer, Berlin, 2001.
[21] L.A. Sklar, B.S. Hudson, R.D. Simoni, Conjugated polyene fatty acids as fluorescent probes: binding to bovine serum albumin, Biochemistry 16 (1977) 5100–5108.
[22] F.L. Cui, J. Fan, D.L. Ma, M.C. Liu, X.G. Chen, Z.D. Hu, A study of the interaction between a new reagent and serum albumin by fluorescence spectroscopy, Anal. Lett. 36 (2003) 2151–2166.
[23] Y. Lu, F. Cui, J. Fan, Y. Yang, X. Yao, J. Li, Interaction of human serum albumin with N-(4-ethoxyphenyl)-N0-(4-antipyrinyl) thiourea using spectroscopies and molecular modelling method, J. Luminesc. 129 (2009) 734–740.
[24] X.M. He, D.C. Carter, Atomic structure and chemistry of human serum albumin, Nature 358 (1992) 209–215.
[25] T. Peters, All About Albumin; Biochemistry, Genetics and Medical Applications, Academic, San Diego, CA, 1995.
[26] J.Y. Lee, M. Hirose, Partially folded state of the disulfide-reduced form of human serum albumin as an intermediate for reversible denaturation, J. Biol. Chem. 267 (1992) 14753–14758.
[27] K.S. Witold, H.M. Henry, C. Dennis, Determination of protein secondary structure by Fourier transform infrared spectroscopy: a critical assessment, Biochemistry 32 (1993) 389–394.
[28] F.L. Cui, J. Fan, J.P. Li, Z. Hu, Interactions between 1-benzoyl-4-p-chlorophenyl thiosemicarbazide and serum albumin: investigation by fluorescence spectroscopy, Bioorg. Med. Chem. 12 (2004) 151–157.